PROCEEDINGS, 44th Workshop on Geothermal Reservoir Engineering
Stanford University, Stanford, California, February 11-13, 2019
SGP-TR-214

A Fractal Gas-Water Relative Permeability Model in Geothermal Reservoirs

Pengliang Yu, Rosalind Archer

Department of Engineering Science, University of Auckland Private Bag 92019 Auckland 1142, New Zealand

pengliang.yu@auckland.ac.nz

Keywords: gas-water distribution, relative permeability, fractal model, surface tension

ABSTRACT

Reliable gas-water relative permeability models are of significance for accurate numerical simulation for both petroleum and geothermal reservoirs. In this study, a modified Hagen-Poiseuille equation for gas/water flow was proposed based on the shell momentum balance method (Bird, 2002) with the water and gas distributed within pores. A gas-water relative permeability model is proposed based on fractal scaling theory. The Young-Laplace equations were employed in the proposed model to capture the mechanical equilibrium of gas and water at different temperatures. The new model has been validated by comparison to various experiments in the literature for steam-water relative permeability in geothermal rock samples. The results show that an increased fractal dimension for pore size distribution increases gas relative permeability but decreases the water relative permeability for a given saturation. However, the tortuosity fractal dimension only shows a significant effect on the water phase relative permeability. In addition, increasing temperature leads to lower surface tension which will then increase the steam relative permeability.

1. INTRODUCTION

Two phase flows in porous media are of great significance to the development of petroleum and geothermal reservoirs. The common used approach to describe a two phase flow is the relative permeability functions, which is based on the Darcy equation. And the accurate relative permeability models are the most useful and necessary methods for capturing the flow mechanisms and predicting the oil/gas recovery and geothermal fluid (steam/water) production.

Many empirical and theoretical models for gas-water relative permeability model have been proposed to describe flow in porous media. the Corey model (1954), the Brooks and Corey model (1964), Verma (1986), the viscous coupling model (Fourar & Lenormand, 1998) etc. are representatives of those models. Horne et al.(2000) found that the steam-water relative permeability in geothermal porous media was similar to the typical relative permeability curves of nitrogen-water. Li and Horne (K. Li, 2004; K. Li & Horne, 2007) proposed a fractal model based on the capillary pressure curves and fractal theory. They derived a more generalized capillary model, which was integrated into Purcell model and Burdine mode to estimate the relative permeability. However, previous models normally ignore the surface geometry of flow channel, the corresponding phase flow structure, and phase interference, which are the main factors that control multiphase flow behavior (Nicholl, Rajaram, & Glass, 2000; Pruess & Tsang, 1990). Chen and Horne (2006) put forward a tortuous channel model, but the parameters in their models are hard to measure. Chima, Geiger (2012) and Y. Li, et al., (2014) proposed their analytical models of relative permeability based on shell momentum balance method (Bird, 2002) using two ideal smooth parallel planes. However, their models only applied to flow in a single pore or fracture and neglected the capillary pressure effect. In addition, those models assumed a constant temperature atmosphere, which is not true in the extraction of petroleum and geothermal fluids.

Multiphase fluid flow processes are governed by the pore-space characteristics such as pore size distribution, tortuosity, connectivity etc., which makes the analytical solution for relative permeability become a challenging task. Fortunately, most naturally porous media including geothermal rocks have been shown to obey fractal scaling laws(Chang & Yortsos, 1990; Sahimi, 1993; Adler, 1996; Yu & Li, 2001; K. Li & Horne, 2003.), and fractal geometry theory has been successfully used to capture the geometrical structures of these so-called fractal porous media. Yu et al.(2002) firstly proposed an analytical expression for the relative permeability of unsaturated bi-dispersed porous media based on fractal capillary bundle model. Then, several researchers extended Yu's fractal model for different cases (X. Chen et al., 2017; Liu, et al., 2007; Xu, et al., 2013). However, studies seldom considered water/gas interference in the channels, and just used the simple cubic law or Hagen-Poiseuille equation to represent the fluid flow process, which is not necessarily suitable for complex flow structures.

In this study, following Bird's (2002) shell momentum balance method, a modified Hagen-Poiseuille equation was obtained by considering the influence of irreducible water, the distribution of gas and water in the pores. Then the modified Hagen-Poiseuille equation and capillary pressure were integrated into the fractal scaling theory to obtain the fractal relative permeability functions which take into account the gas/water distribution, the pore size distribution, pore tortuosity as well as the capillary pressure in variable temperature situations. Experimental data was used to validate the proposed models followed by the analysis of the effect of fractal characteristics and variable temperature on characteristics of the gas-water relative permeability.

Yu and Archer.

2. MATHEMATICAL MODELING

2.1 Fractal scaling laws of porous media

Fractal scaling laws have been found in petroleum and geothermal rocks (Chang & Yortsos, 1990; Sahimi, 1993; Adler, 1996; Yu & Li, 2001; K. Li & Horne, 2003). On the basis of the fractal scaling theory, the cumulative pore size distribution can be reasonably characterized by the following equation (Yu & Cheng, 2002):

$$N(\delta > r) = \left(\frac{r_{\max}}{r}\right)^{D_f} \tag{1}$$

Where N is the pore's number; r and r_{max} are the radius of a certain pore and the maximum pore, respectively; δ is the length scale; The fractal dimension for pore size distribution is in the range of $0 < D_f < 2$ and $0 < D_f < 3$ in two and three dimensions, respectively. It can be determined by the following equation (Yu & Li, 2001):

$$D_f = d - \frac{\ln \varphi}{\ln\left(r_{\min}/r_{\max}\right)} \tag{2}$$

Where d is the Euclidean dimension, and d =2 and 3 in two and three dimensions; φ is the porosity; r_{min} is the minimum pore radius. r_{max} is the maximum pore radius. In general, Eq. (1) can be regarded as a continuous and differentiable equation if we assume the pores in the porous media are numerous. After differentiating Eq. (1), the total number of pores from the range r to $r + dr$ are(Yu & Li, 2001;Yu & Cheng, 2002):

$$-dN = D_f r_{\max}^{D_f} r^{-(D_f+1)} dr \tag{3}$$

The probability density function for cumulative pore distribution in the porous media can be expressed as (Yu & Cheng, 2002; Xu, et al., 2013):

$$f(r) = D_f r_{\min}^{D_f} r^{-(D_f+1)} \tag{4}$$

The probability density function should satisfy the normalizing condition(Yu & Li, 2001;Yu & Cheng, 2002): $\int_{r_{\min}}^{r_{\max}} f(r) = 1$, this results in $\left(r_{\min}/r_{\max}\right)^{D_f} = 0$, which indicates that $r_{\min}$ □ must be satisfied for the fractal analysis of porous media.

The flow path in a porous medium is often reasonably idealized as tortuous capillaries/tubes with different cross-sectional sizes. Owing to the tortuous nature of those capillaries. The practical length of that $L > L_0$, where L_0 is the representative length of the representative elementary volume (REV). based on the self-similar fractal law, the length L(r) and representative length follows the relationship (Yu & Cheng, 2002):

$$L(r) = (2r)^{1-D_T} L_0^{D_T} \tag{5}$$

Where $1<D_T<2$ (or $1<D_T<3$) is the tortuosity fractal dimension in the space of two (or three) dimensions. Notably, the higher the value of D_T, the more tortuous of the flow path is.

2.2 Modified Hagen-Poiseuille equation for gas and water phase in porous media

A series of tortuous capillary channels is used to represent the flow paths in isotropic porous media, whose size and length distributions obey statistically fractal scaling laws. For the capillaries with different radius r, there exists a critical value r_c, wetting fluids (water) fully saturated the pores of radius $r \leq r_c$, whereas two phase (gas and water) flow instantaneously in the pores whose size $r \geq r_c$ (Fig.1) The H-P equation is a classical physical law for characteristic the Newtonian fluid laminar flow through a single capillary with ideal circular tube. The original Hagen-Poiseuille equation cannot reflect the flow mechanism with the existence of absorbed water layer in the porous media (Izadi & Ghalambor, 2013). In order to get the flow equation of gas and water in the tube with the existence of bound water, we apply momentum balance and Newton's law of viscosity to the pore configuration and the flow configuration shown in Fig.2, leading to the following modified Hagen-Poiseuille equation for water and gas respectively. The detailed mathematical derivation is given in Appendix A.

For water flow rates in a porous with radius of r could be expressed as:

$$q_{w1} = \frac{(p_0 - p_L)\pi}{8\mu_w L}(1 - S_{wc})^2 r^4 \quad r_{min} \le r \le r_c \tag{6a}$$

$$q_{w2} = \frac{(p_0 - p_L)\pi}{8\mu_w L}(S_w - S_{wc})^2 r^4 \quad r_c \le r \le r_{max} \tag{6b}$$

For gas flow in porous media, the flow rates could be calculated by:

$$q_g = \frac{(p_0 - p_L)\pi}{8\mu_g L}(1 - S_w)^2 r^4 + \frac{(p_0 - p_L)\pi}{4\mu_w L}(1 - S_w)(S_w - S_{wc}) r^4 \quad r_c \le r \le r_{max} \tag{6c}$$

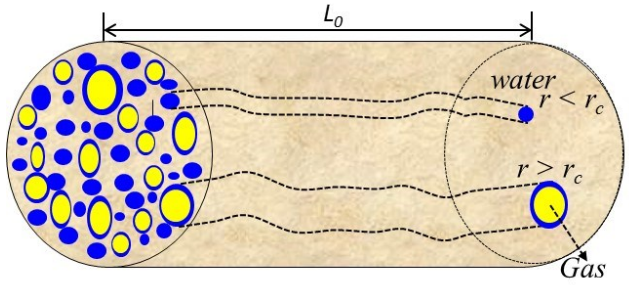

Figure 1 Physical conceptual model of gas-water flow in porous media

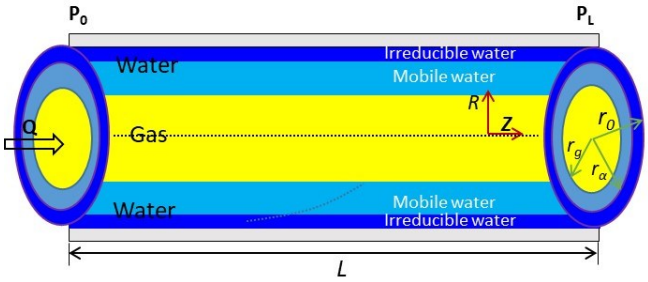

Figure 2 Ideal circular tube to be used in the mathematical model representing porous media with radius r ≥r_c

2.3 Gas-water relative permeability

According to the illustration in section 2.2, the water volumetric flow rates in the capillaries are the sum of single phase flow within pores of radius $r < r_c$, and the flow around the surface in the pores with the radius $r > r_c$, so the water volumetric flow rates in all pores of porous media can be expressed as:

$$Q_w = \int_{r_{min}\sqrt{1-S_{wc}}}^{r_c\sqrt{1-S_{wc}}} q_{w1}(-dN) + \int_{r_c\sqrt{S_w-S_{wc}}}^{r_{max}\sqrt{S_w-S_{wc}}} q_{w2}(-dN)$$

$$= \frac{\pi D_f r_{max}^{D_f}(p_0 - p_L)}{2^{4-D_T} L_0^{D_T} \mu_w}\left[(1 - S_{wc})^{\frac{7-D_f+D_T}{2}} \frac{r_c^{3-D_f+D_T} - r_{min}^{3-D_f+D_T}}{3 - D_f + D_T} + (S_w - S_{wc})^{\frac{7-D_f+D_T}{2}} \frac{r_{max}^{3-D_f+D_T} - r_c^{3-D_f+D_T}}{3 - D_f + D_T}\right] \tag{7a}$$

Similarly, the gas phase flows through the capillaries in the radius from r_c to r_{max}; hence, the total steam volumetric flow rates can be obtained as:

$$Q_g = \int_{r_c\sqrt{1-S_w}}^{r_{\max}\sqrt{1-S_w}} q_g\left(-dN\right)$$
$$= \frac{\pi D_f r_{\max}^{D_f}\left(p_0 - p_L\right)}{2^{4-D_T} L_0^{D_T}}\left[\frac{\left(1-S_w\right)^{\frac{7-D_f+D_T}{2}}}{\mu_g} + \frac{2\left(1-S_w\right)^{\frac{7-D_f+D_T}{2}}\left(S_w - S_{wc}\right)}{\mu_w}\right]\frac{r_{\max}^{3-D_f+D_T} - r_c^{3-D_f+D_T}}{3-D_f+D_T} \tag{7b}$$

The flow rates through the two phase system can be also given by Darcy's extended law:

$$Q_w = -\frac{K_w A_s \Delta p_w}{\mu_w L_0} \tag{8a}$$

$$Q_g = -\frac{K_g A_s \Delta p_g}{\mu_g L_0} \tag{8b}$$

Where A_s is the total pore area, K_g denotes the effective permeability of gas and K_w for water. The pressure drop in water and steam phase without considering the temperature changes can be expressed by:

$$\Delta p_w = \frac{p_0 - p_L}{S_w} \tag{9a}$$

$$\Delta p_g = \frac{p_0 - p_L}{1-S_w} \tag{9b}$$

Due to the change of temperature in the capillary, the term Δp_g should be changed to $\Delta p_g'$. Therefore, Eq. (8b) should be transformed to the following equation:

$$Q_g = -\frac{K_g A_s \Delta p_g'}{\mu_g L_0} \tag{10}$$

The relationship between Δp_g and $\Delta p_g'$ is: (For a detailed derivation of Eq. (11), please see Appendix B)

$$\frac{\Delta p_g'}{\Delta p_g} = \frac{2\sigma_2}{\sigma_1} - 1 \tag{11}$$

Combining the above equations, one could get the expressions of effective water and gas permeability in the porous media respectively:

$$K_w = \frac{\pi D_f r_{\max}^{D_f} S_w}{2^{4-D_T} L_0^{D_T-1} A_s}\left[\left(1-S_{wc}\right)^{\frac{7-D_f+D_T}{2}}\frac{r_c^{3-D_f+D_T} - r_{\min}^{3-D_f+D_T}}{3-D_f+D_T} + \left(S_w - S_{wc}\right)^{\frac{7-D_f+D_T}{2}}\frac{r_{\max}^{3-D_f+D_T} - r_c^{3-D_f+D_T}}{3-D_f+D_T}\right] \tag{12a}$$

$$K_g = \frac{\pi D_f r_{\max}^{D_f} S_g}{2^{4-D_T} L_0^{D_T-1} A_s}\frac{\sigma_1}{2\sigma_2 - \sigma_1}\left[\left(1-S_w\right)^{\frac{7-D_f+D_T}{2}} + \frac{2\mu_g\left(1-S_w\right)^{\frac{7-D_f+D_T}{2}}\left(S_w - S_{wc}\right)}{\mu_w}\right]\frac{r_{\max}^{3-D_f+D_T} - r_c^{3-D_f+D_T}}{3-D_f+D_T} \tag{12b}$$

The absolute permeability of the reservoir rock satisfied the condition of S_w=1, which means all the capillaries are filled with the single water phase. It can be expressed as:

$$K = \frac{\pi D_f r_{\max}^{D_f}}{2^{4-D_T} L_0^{D_T-1} A_s} \frac{r_{\max}^{3-D_f+D_T} - r_{\min}^{3-D_f+D_T}}{3-D_f+D_T} \tag{13}$$

The water saturation can be expressed by:

$$S_w = \frac{\int_{r_{\min}}^{r_c} \pi r^2 D_f r_{\max}^{D_f} r^{-(D_f+1)} dr + \int_{r_c\sqrt{S_w}}^{r_{\max}\sqrt{S_w}} \pi\left(r^2 - S_g r^2\right) D_f r_{\max}^{D_f} r^{-(D_f+1)} dr}{\int_{r_{\min}}^{r_{\max}} \pi r^2 D_f r_{\max}^{D_f} r^{-(D_f+1)} dr} \tag{14}$$

Combining Eq. (2) in the case of d=2 with Eq. (14) results in:

$$\frac{r_c}{r_{\max}} = \left[\frac{(1-\phi)S_w + \phi - S_w^{\frac{4-D_f}{2}}}{1 - S_w^{\frac{4-D_f}{2}}}\right]^{\frac{1}{2-D_f}} \tag{15}$$

Therefore, the water relative permeability expressions can be obtained by:

$$K_{rw} = S_w\left[\left(1-S_{wc}\right)^{\frac{7-D_f+D_T}{2}} - \left(S_w - S_{wc}\right)^{\frac{7-D_f+D_T}{2}}\right]\left[\frac{(1-\phi)S_w + \phi - S_w^{\frac{4-D_f}{2}}}{1 - S_w^{\frac{4-D_f}{2}}}\right]^{\frac{3-D_f+D_T}{2-D_f}} + S_w\left(S_w - S_{wc}\right)^{\frac{7-D_f+D_T}{2}} \tag{16a}$$

$$K_{rg} = S_g \frac{\sigma_1}{2\sigma_2 - \sigma_1}\left\{1 - \left[\frac{(1-\phi)S_w + \phi - S_w^{\frac{4-D_f}{2}}}{1 - S_w^{\frac{4-D_f}{2}}}\right]^{\frac{3-D_f+D_T}{2-D_f}}\right\}\left[\left(1-S_w\right)^{\frac{7-D_f+D_T}{2}} + \frac{2\mu_g\left(1-S_w\right)^{\frac{7-D_f+D_T}{2}}\left(S_w - S_{wc}\right)}{\mu_w}\right] \tag{16b}$$

The surface tension of pure liquid water in contact with its vapor has been given by IAPWS (Wagner & Pruß, 2002) as:

$$\sigma = 235.8\left(1-\frac{T}{T_c}\right)^{1.256}\left[1 - 0.625\left(1-\frac{T}{T_c}\right)\right]$$

Where T and T_c are the temperature of water-steam system and critical temperature respectively. The critical temperature T_c = 647.096K.

3 MODEL VALIDATION AND PARAMETER ANLYSIS

3.1 Model Validation

In order to validate our proposed model, the results calculated by our model Eq. (16) are compared with experimental data from literature studies. Sanchez and Schechter (1990) conducted the steam-water relative permeability experiments in an unconsolidated core sample under steady-state, adiabatic conditions. Then, Satik (1998) and Mahiya and Horne (1999) performed several experiments for steam water flow on Berea sandstone to obtain relative permeability with steady-state method combined with X-ray CT scanner. Chen and Horne (2007) did several steam water flow experiments in smooth and rough walled circular glass at isothermal condition using improved experimental techniques. From Fig.3, we can find that the results predicted by our model are consistent with experimental results from different sources.

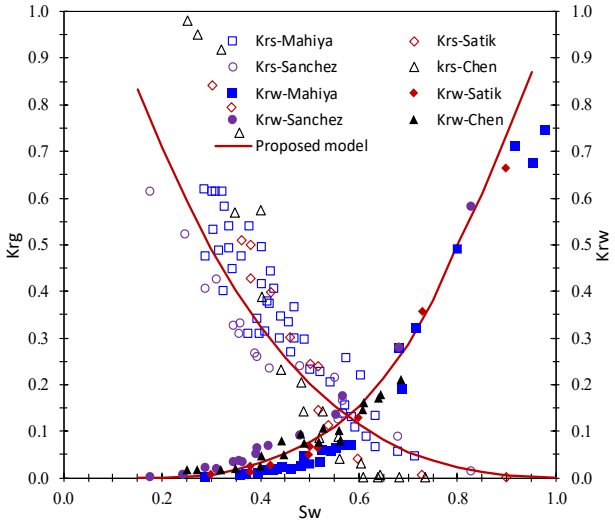

Figure 3 A comparison between the relative permeability predicted by proposed model and experiments data (Sanchez 1990; Satik 1998; Mahiya and Horne 1999; Chen and Horne 2007)

3.2 Sensitive Analysis

The relative permeability for gas and water phase in unsaturated porous media under different fractal dimensions predicted from Eq.16 are plotted in Fig.4 and Fig.5. As we see in Fig. 4, the increased fractal dimension D_f would increase the gas phase relative permeability at a specific S_w, in contrast, the relative permeability of water decreases when D_f increases. This is because a higher D_f represents a larger proportion of small pores, which will lead to a smaller critical pore radius for a given saturation S_w. As a result, increased capillary pressure then enhances the gas relative permeability and decreases the water relative permeability accordingly.

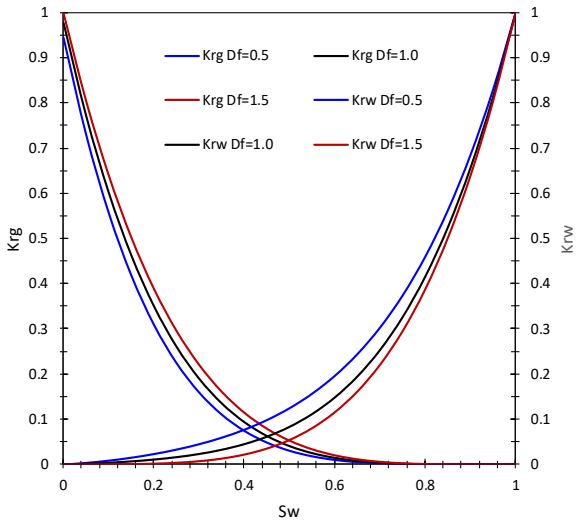

Figure 4 Impact of fractal dimensions for pore size distribution on relative permeability (D_T=1.1, ϕ=0.3, S_{we}=0, T_1=T_2)

As shown in Fig.5, increased tortuosity fractal dimension decreased the relative permeability of both gas and water phase for the reason that the larger value of tortuosity fractal dimension indicates highly tortuous flow path, which would enhance the flow resistance. Therefore, both gas and water relative permeability will decrease with increasing D_T, however, the effect of D_T on water phase relative permeability is larger than its effect on gas relative permeability. This is because for gas core flow in the capillaries, the impact of tortuous capillary channel on the water flow is greater than gas flow, which results in the less significant effect on gas relative permeability.

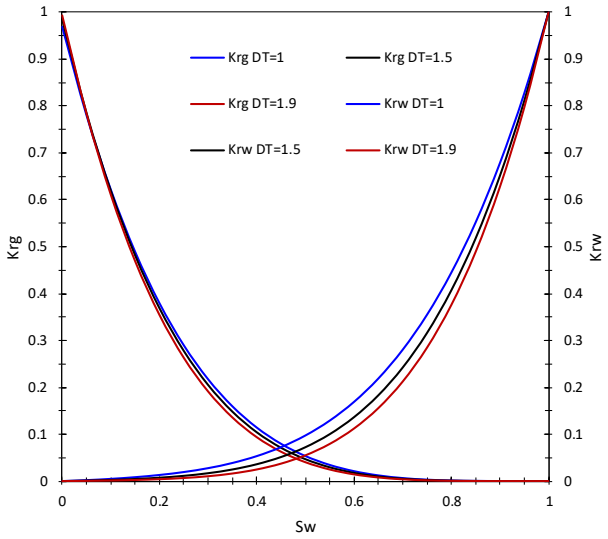

Figure 5 Impact of fractal dimensions for tortuosity on the relative permeability (D_f=1.2, ϕ=0.3, S_{wc}=0, T_1=T_2)

Fig.6 illustrates the effect of temperature on the relative permeability of gas and water in unsaturated porous media. With increasing temperature, the gas relative permeability increases due to the decrease of surface tension, and the gas relative permeability could be larger than 1 for higher temperature situation. This is because decreasing surface tension means there is less interaction between gas and water and the overall resistance to gas flow along the channel would decrease which leads to the gas flow core moving faster in the capillary channel. However, the influence of temperature on water relative permeability could be neglected as shown in Fig.6.

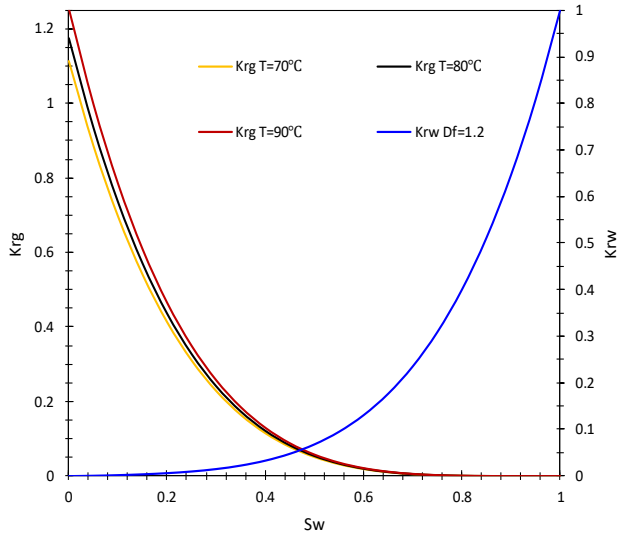

Figure 6 Impact of temperature (surface tension) on the relative permeability (D_f=1.2, D_T=1.1, ϕ=0.3, S_{wc}=0, reference temperature T_1=20°C)

CONCLUSION

Based on shell momentum balance methods, the modified Hagen-Poiseuille equation for gas and water phase was proposed for considering the gas and water distribution in the capillary. A fractal relative permeability model was derived by coupling the modified Hagen-Poiseuille equation, the mechanical equilibrium of steam and water at different temperatures and the fractal scaling laws. The new model was validated by various experiments data, which showed good agreement with those data. According to this study, it has been found that the gas-water flow process in porous media are governed by the gas/water distribution, capillary pressure, temperature as well as geometrical parameters of porous media. The fractal parameter analysis shows that the increased pore size distribution fractal dimension would increase the gas phase permeability but reduce the water phase permeability. Although the tortuosity fractal dimension can simultaneously decrease the relative permeability for water and gas, the effect of tortuosity fractal dimension on gas relative permeability is smaller than its effect on water relative permeability. In addition, the gas relative permeability would increase with the increase of temperature. The proposed model could help understanding the gas/water transport mechanisms in the fractal porous media.

Yu and Archer.

NOMENCLATURE

Normal

A_s	Area of flow channel
d	Euclidean dimension
D_f	Fractal dimension for pore size distribution
$f(r)$	Probability density function for pore size distribution
K	Absolute permeability (m^2)
K_g	Effective permeability for the steam phase (m^2)
K_{rg}	Relative permeability for the steam phase
K_{rw}	Relative permeability for the water phase
K_w	Effective permeability for the water phase (m^2)
L	The length of the capillary
N	Pore's number
p_0	Pressure on flow cross section in z=0
p_L	Pressure on flow cross section in z=L
p_g	Steam pressure (Pa)
p_{g1}	Steam phase pressure on flow cross section in z=0
p_{g2}	Steam phase pressure on flow cross section in z=L
p_w	Water pressure (Pa)
p_{w1}	Water phase pressure on flow cross section in z=0
p_{w2}	Water phase pressure on flow cross section in z=L
Δp_g	Differential pressure between p_{g1} and p_{g2} (Pa)
Δp_w	Differential pressure between p_{w1} and p_{w2} (Pa)
q_g	Steam flow rates of the single capillary (m^3/s)
Q_g	Steam flow rates of the porous media (m^3/s)
q_w	Water flow rates of the single capillary (m^3/s)
Q_w	Water flow rates of the porous media (m^3/s)
r	The radius of a certain pore (m)
r_a	The thickness of mobile water region (m)
r_0	The radius of pore (m)
r_c	Critical pore radius for the porous media(m)
r_g	The thickness of steam region (m)
r_{max}	The maximum pore radius (m)
r_{min}	The minimum pore radius (m)
S_w	Water saturation

S_{wc} irreducible water saturation

S_{wm} mobile water saturation

T Absolute Temperature (T)

V_z^g Velocity of steam phase

V_z^w Velocity of water phase

Greeks

μ_g The dynamic viscosity for steam region (Pa.s)

μ_w The dynamic viscosity for water region (Pa.s)

δ Length scale

ρ_w water density (Kg/m^3)

φ Porosity

τ_{rz} Force in the z direction on a unit area perpendicular to the r direction

τ_{rz}^w Force in the z direction on a unit area perpendicular to the r direction in the mobile water

τ_{rz}^g Force in the z direction on a unit area perpendicular to the r direction in the gas

APPENDIX A

The modeled porous media geometry was assumed a tube and flow configuration are shown in Fig.2 within the pipe, the flow of water and gas are assumed to satisfied the following assumptions:

a. Both gas and water are Newtonian fluid

b. Gas is compressible and water is slightly compressible, both have constant properties

c. The pore throat is treated as pipe and the flow in a pipe takes into account of the gas core fluid

d. The irreducible water is absorbed on the walls of pores and distributed uniformly on the walls

e. The flow is laminar and in steady-state.

f. The pipe is oriented at horizontal, fluid gravity and buoyancy effects are neglected

Following the Bird's (2002) method, perform momentum balance within a capillary shown in Fig.2 yields:

Apply the shell momentum balance (Bird, 2002) in the capillary shown in figure1yields:

$$\left(2\pi rL\tau_{rz}\right)\Big|_r - \left(2\pi rL\tau_{rz}\right)\Big|_{r+\Delta r} + 2\pi r\cdot\Delta r\cdot\left(p_0 - p_L\right) = 0 \tag{A1}$$

When we divide the Eq. (A1) by L and take the limit as $\Delta r \to 0$, we get

$$\lim_{\Delta r\to 0}\left(\frac{\left(r\tau_{rz}\right)_{r+\Delta r} - \left(r\tau_{rz}\right)_{r+\Delta r}}{\Delta r}\right) = \frac{p_0 - p_L}{L}r \tag{A2}$$

Eq. (A2) can be simplified to:

$$\frac{\partial\left(r\tau_{rz}\right)}{\partial r} = \frac{p_0 - p_L}{L}r \tag{A3}$$

Eq. (A3) applies for both gas (g) phase and water (w) phase. Integration of equation of Eq. (A3) for these regions gives:

For mobile water phase:

$$\tau_{rz}^{w} = \left(\frac{p_0 - p_L}{2L} \right) r + \frac{C_1^w}{r} \tag{A4}$$

For gas phase:

$$\tau_{rz}^{g} = \left(\frac{p_0 - p_L}{2L} \right) r + \frac{C_1^g}{r} \tag{A5}$$

When Newton's law of viscosity (R. B. Bird, 2002) is substituted into Eq. (A4) and (A5) we get:

For mobile water phase:

$$-\mu_w \frac{\partial V_z^w}{\partial r} = \left(\frac{p_0 - p_L}{2L} \right) r + \frac{C_1^w}{r} \tag{A6}$$

$$V_z^w = -\left(\frac{p_0 - p_L}{4\mu_w L} \right) r^2 - \frac{C_1^w}{\mu_w} \ln r + C_2^w \tag{A7}$$

For gas phase:

$$-\mu_g \frac{\partial V_z^g}{\partial r} = \left(\frac{p_0 - p_L}{2L} \right) r + \frac{C_1^g}{r} \tag{A8}$$

$$V_z^g = -\left(\frac{p_0 - p_L}{4\mu_g L} \right) r^2 - \frac{C_1^g}{\mu_g} \ln r + C_2^g \tag{A9}$$

Then, define boundary conditions to solve the above equations.

Boundary condition 1: $\left. \frac{\partial V_z^g}{\partial r} \right|_{r=0} = 0$

Boundary condition 2: $V_z^g \Big|_{r=r_g} - V_z^w \Big|_{r=r_g} = 0$

Boundary condition 3: $V_z^w \Big|_{r=r_\alpha} = 0$

Boundary condition 4: $\tau_{rz}^g \Big|_{r=r_g} = \tau_{rz}^w \Big|_{r=r_g}$

Solving $C_1^w, C_2^w, C_1^g, C_2^g$ in the Eq.(A8) and (A9) with boundary conditions, we get:

$$V_z^w = -\frac{p_0 - p_L}{4\mu_w L} r^2 + \frac{p_0 - p_L}{4\mu_w L} r_\alpha^2 \tag{A8a}$$

$$V_z^g = -\frac{p_0 - p_L}{4\mu_g L} r^2 + \frac{p_0 - p_L}{4\mu_g L} r_g^2 + \frac{p_0 - p_L}{4\mu_w L}\left(r_\alpha^2 - r_g^2\right) \tag{A8b}$$

Integrating Eq. (A8a) and (A8b) over the range of each region in the capillary tube, the gas and water flow equation can be expressed, respectively:

$$q_w = \int_{r_g}^{r_\alpha} 2\pi r V_z^w dr = \frac{(p_0 - p_L)\pi}{8\mu_w L}\left(r_\alpha^2 - r_g^2\right)^2 \tag{A9a}$$

$$q_g = \int_0^{r_g} 2\pi r V_z^g dr = \frac{(p_0 - p_L)\pi}{8\mu_g L} r_g^4 + \frac{(p_0 - p_L)\pi}{4\mu_w L}\left(r_\alpha^2 r_g^2 - r_g^4\right) \tag{A9b}$$

For the circular geometry and flow configuration shown in Fig.2, we could get the correlations: $\frac{r_g^2}{r_0^2} = S_g$, $\frac{r_\alpha^2}{r_0^2} = 1 - S_{wc}$, $\frac{r_g^2}{r_\alpha^2} = \frac{S_g}{1 - S_{wc}}$, therefore, water and steam flow rates in porous medium be expressed as:

$$q_{w1} = \frac{(p_0 - p_L)\pi}{8\mu_w L}\left(1 - S_{wc}\right)^2 r^4 \quad r_{min} \le r \le r_c \tag{A10a}$$

$$q_{w2} = \frac{(p_0 - p_L)\pi}{8\mu_w L}\left(S_w - S_{wc}\right)^2 r^4 \quad r_c \le r \le r_{max} \tag{A10b}$$

$$q_g = \frac{(p_0 - p_L)\pi}{8\mu_g L}(1 - S_w)^2 r^4 + \frac{(p_0 - p_L)\pi}{4\mu_w L}(1 - S_w)\left(S_w - S_{wc}\right) r^4 \quad r_c \le r \le r_{max} \tag{A10c}$$

APPENDIX B

Here, we employ the Laplace equation to describe the difference of Δp_g and $\Delta p_g'$ in the case of considering temperature change in the porous media. Applying Young-Laplace equation to the hemispherical portion of the steam-water interface in different temperatures, shown in Fig.7, we obtain:

$$p_{g2} - p_{w2} = \frac{2\sigma_1}{r} \tag{B1}$$

$$p'_{g2} - p_{w2} = \frac{2\sigma_2}{r} \tag{B2}$$

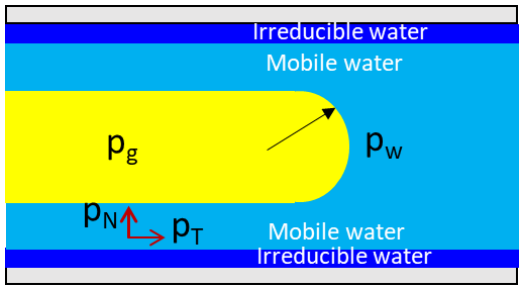

Figure7 Schematic of force analysis of bubble inside a water filled tube

For the mechanical equilibrium of the cylindrical portion, due to the existence of disjoining pressure, Pw $\neq P_N = P_T$. P_N satisfy the expression (Verma, 1986; Chatterjee, et al, 2011; Israelachvili, 2011):

$$p_N - p_w = \frac{\sigma_1}{r} \tag{B3}$$

Therefore, in the inlet of the tube, the water pressure and steam pressure satisfy the equation:

$$p_{v1} - p_{w1} = \frac{\sigma_1}{r} \tag{B4}$$

Integrate equations from Eq. B1 to Eq. B4, one could get:

$$\frac{\Delta p'_g}{\Delta p_g} = \frac{\frac{\sigma_1}{r} - \frac{2\sigma_2}{r} + \Delta p'_w}{-\frac{\sigma_1}{r} + \Delta p_w} \tag{B5}$$

As the pressure differences of liquid with and without temperature changes are nearly constant, in there, we assume $\Delta p'_w \approx \Delta p_w$, Based on this assumption, we could get the ratio between Δp_g and $\Delta p'_g$:

$$\frac{\Delta p'_g}{\Delta p_g} = \frac{2\sigma_2}{\sigma_1} - 1 \tag{B6}$$

REFERENCES

Adler, P. M. (1996). Transports in fractal porous media. *Journal of Hydrology*, *187*(1–2), 195–213. https://doi.org/10.1016/S0022-1694(96)03096-X

Bird, R. B., Stewart, W. E., & Lightfoot, E. N. (2002). *Transport phenomena*. J. Wiley&Sons, Inc.

Brooks, R. H., & Corey, A. T. (1964). Hydraulic properties of porous media. *Hydrology Papers, Colorado State University. Fort Collins CO*, *3*(3), 27 pgs. https://doi.org/citeulike-article-id:711012

Chang, J., & Yortsos, Y. C. (1990). Pressure Transient Analysis of Fractal Reservoirs. *SPE Formation Evaluation*, *5*(01), 31–38. https://doi.org/10.2118/18170-PA

Chatterjee, A., Plawsky, J. L., & Wayner, P. C. (2011). Disjoining pressure and capillarity in the constrained vapor bubble heat transfer system. *Advances in Colloid and Interface Science*. https://doi.org/10.1016/j.cis.2011.02.011

Chen, C.-Y., Li, K., & Horne, R. (2007). *Experimental Study of Phase-Transformation Effects on Relative Permeabilities in Fractures*. *SPE Reservoir Evaluation & Engineering* (Vol. 10). https://doi.org/10.2118/90233-PA

Chen, C. Y., & Horne, R. N. (2006). Two-phase flow in rough-walled fractures: Experiments and a flow structure model. *Water Resources Research*, *42*(3). https://doi.org/10.1029/2004WR003837

Chen, X., & Yao, G. (2017). An improved model for permeability estimation in low permeable porous media based on fractal geometry and modified Hagen-Poiseuille flow. *Fuel*, *210*, 748–757. https://doi.org/10.1016/J.FUEL.2017.08.101

Chima, A., Chavez Iriarte, E. A., & Calderon Carrillo, Z. H. (2010). An Equation To Predict Two-Phase Relative Permeability Curves in Fractures. In *SPE Latin American and Caribbean Petroleum Engineering Conference*. https://doi.org/10.2118/138282-MS

Corey, A. T. (1954). The Interrelation Between Gas and Oil Relative Permeabilites. *Producers Monthly*, *19*(1), 38–41.

Fourar, M., & Lenormand, R. (1998). A Viscous Coupling Model for Relative Permeabilities in Fractures. *Proceedings of SPE Annual Technical Conference and Exhibition*, (1), 6. https://doi.org/10.2118/49006-MS

Horne, R. N., Satik, C., Mahiya, G., Li, K., Ambusso, W., Tovar, R., … Nassori, H. (n.d.). Steam-Water Relative Permeability. Retrieved from http://ekofisk.stanford.edu/geotherm.html

Israelachvili, J. (2011). *Intermolecular and Surface Forces*. *Intermolecular and Surface Forces*. https://doi.org/10.1016/C2009-0-21560-1

Izadi, M., & Ghalambor, A. (2013). New Approach in Permeability and Hydraulic-Flow-Unit Determination. *SPE Reservoir Evaluation & Engineering*, *16*(03), 257–264. https://doi.org/10.2118/151576-PA

Li, K. (2004). Generalized Capillary Pressure and Relative Permeability Model Inferred from Fractal Characterization of Porous Media. In *SPE Annual Technical Conference and Exhibition*. https://doi.org/10.2118/89874-MS

Li, K., & Horne, R. N. (2003). *Fractal Characterization of The Geysers Rock*. *Geothermal Resources Council Transactions* (Vol. 27). Retrieved from http://pangea.stanford.edu/~kewenli/grc2003_fractal.pdf

Li, K., & Horne, R. N. (2007). Systematic study of steam-water capillary pressure. *Geothermics*, *36*, 558–574. https://doi.org/10.1016/j.geothermics.2007.08.002

Li, Y., Li, X., Teng, S., & Xu, D. (2014). Improved models to predict gasewater relative permeability in fractures and porous media. *Journal of Natural Gas Science and Engineering*, *19*, 190–201. https://doi.org/10.1016/j.jngse.2014.05.006

Liu, Y., Yu, B., & Xiao, B. (2007). *A FRACTAL MODEL FOR RELATIVE PERMEABILITY OF UNSATURATED POROUS MEDIA WITH CAPILLARY PRESSURE EFFECT*. *Fractals* (Vol. 15). Retrieved from www.worldscientific.com

Mahiya, G. F. (1999). *Experimental measurement of steam-water relative permeability*. *Petroleum Engineering* (Vol. Master). Retrieved from https://earthsci.stanford.edu/ERE/research/geoth/publications/techreports/SGP-TR-164.pdf

Majumdar, A., & Bhushan, B. (1990). Role of Fractal Geometry in Roughness Characterization and Contact Mechanics of Surfaces. *Journal of Tribology*, *112*(2), 205. https://doi.org/10.1115/1.2920243

Nicholl, M. J., Rajaram, H., & Glass, R. J. (2000). Factors controlling satiated relative permeability in a partially-saturated horizontal fracture. *Geophysical Research Letters*, *27*(3), 393–396. https://doi.org/10.1029/1999GL006083

Pruess, K., & Tsang, Y. W. (1990). On two-phase relative permeability and capillary pressure of rough-walled rock fractures. *Water Resources Research*, *26*(9), 1915–1926. https://doi.org/10.1029/WR026i009p01915

Sahimi, M. (n.d.). *Flow phenomena in rocks: from continuum models to fractals, percolation, cellular automata, and simulated annealing*. Retrieved from https://journals.aps.org/rmp/pdf/10.1103/RevModPhys.65.1393

Sanchez, J. M., & Schechter, R. S. (1990). Steady Adiabatic, Two-Phase Flow of Steam and Water Through Porous Media. *SPE Reservoir Engineering*, *5*(03), 293–300. https://doi.org/10.2118/16967-PA

Satik, C. (1998). A Measurement of Steam-Water Relative Permeability. *Engineering*, 120–126. Retrieved from http://citeseerx.ist.psu.edu/viewdoc/download;jsessionid=28D6A49C0189715B9DB47F46FB881D24?doi=10.1.1.586.2573&rep=rep1&type=pdf

Verma, A. (1986). *Effects of phase transformation of steam-water relative permeabilities: Report LBL - 20594*. *U.S. Department of Energy*. Retrieved from https://digital.library.unt.edu/ark:/67531/metadc1093995/m2/1/high_res_d/5540005.pdf

Wagner, W., & Pruß, A. (2002). The IAPWS Formulation 1995 for the Thermodynamic Properties of Ordinary Water Substance for General and Scientific Use. *Journal of Physical and Chemical Reference Data*, *31*(2), 387–535. https://doi.org/10.1063/1.1461829

Xu, P., Qiu, S., Yu, B., & Jiang, Z. (2013). Prediction of relative permeability in unsaturated porous media with a fractal approach. *International Journal of Heat and Mass Transfer*, *64*, 829–837. https://doi.org/10.1016/j.ijheatmasstransfer.2013.05.003

Yu, B., & Cheng, P. (2002). A fractal permeability model for bi-dispersed porous media. *International Journal of Heat and Mass Transfer*, *45*(14), 2983–2993. https://doi.org/10.1016/S0017-9310(02)00014-5

YU, B., & LI, J. (2001). SOME FRACTAL CHARACTERS OF POROUS MEDIA. *Fractals*, *09*(03), 365–372. https://doi.org/10.1142/S0218348X01000804